Distinct 3-dimensional features of immature and mature dendritic cells

Manutsavee Khonlak[1], Donruedee Sanguansermsri[1], Sutatip Pongcharoen[2] and Apirath Wangteeraprasert[2]*

[1]Faculty of Medical Science, Naresuan University, Phitsanulok, 65000, Thailand

[2]Faculty of Medicine, Naresuan University, Phitsanulok, 65000, Thailand

* Corresponding author: apirathw@nu.ac.th

Received: 16 December 2022; Revised: 24 April 2023; Accepted: May 2023

Abstract

Dendritic cells (DCs) are interesting immune cells as they are antigen-presenting cells that initiate the adaptive immune response by T cells. The DCs are categorized as immature and mature DCs based on their morphology and cell surface molecules. In this present study, we employed 3-dimensional (3D) holotomography microscopy to study the morphology and intracellular lipid of DCs. The dendritic cells were derived from peripheral blood monocytes, which were purified from human buffy coats. Immature and mature DCs were characterized by flow cytometry using specific antibodies against cell surface molecules. The results showed that the mature DCs expressed a higher percentage of CD80 (61%) and CD86 (90%) than immature DCs (5% and 9%). Both immature and mature monocyte-derived DCs (mDCs) morphology and intracellular lipid were inspected using 3D holotomography microscopy. The mature mDCs had an increase in cell mass compared to immature mDCs, which were 651.52±43.34 and 465.51±97.87, respectively, $p = 0.158$). The mature mDCs also had an increase in lipid mass compared to immature mDCs, which were 186.57±29.53 and 2.07±0.32, respectively, $p = 0.003$). The data based on this new 3D holotomography could help us extend our understanding of the morphological feature and intracellular lipid profiles of mDCs.

Keywords: dendritic cells, 3-D image, holotomography

Introduction

Dendritic cells (DCs) are interesting immune cells because they function as professional antigen-presenting cells which help start T cell activation in the adaptive immune response (Randolph, Jakubzick, & Qu, 2008; Steinman, 2007). For decades, DCs have been studied as immunotherapy for cancer (Banchereau & Palucka, 2005; Constantino, Gomes, Falcão, Cruz, & Neves, 2016). However, the percentage of DCs in blood circulation is low. To obtain a sufficient amount of DCs for further research, monocytes from peripheral blood are often used to generate monocyte-derived DCs (mDCs).

DCs have been classified, according to their maturation stages, to be immature and mature DCs. The morphology of both stages of DCs has been studied under various types of microscopy. The immature DCs have a round and smooth surface, whereas the mature DCs have an increased size, rough surface, and pseudopodia (Kim & Kim, 2019; Xing, Wang, Hu, & Liu, 2011). The well-known surface markers used to identify the mature DCs are CD80 and CD86, both of which are more highly expressed than in the immature DCs. (Andreae, Piras, Burdin, & Triebel, 2002; Kim & Kim, 2019). Upon DCs maturation, lipids have been reported to be involved in DCs differentiation. This includes, for example, stimulation with lipids such as lipopolysaccharides (LPS), a glycolipid found in the outer membranes of gram-negative bacteria (Thurnher, 2007). Moreover, the mature DCs also have more lipid accumulation inside the cells, which was demonstrated by fluorescence staining or Oil Red O staining (Arai, Soda, Okutomi, & Ishii, 2018). Although the cell morphology and the expression of cell surface molecules of these two stages of DCs have been reported (Verdijk et al., 2004), in this present

study we illustrated the morphology of mDCs using a 3-dimensional (3D) holotomography (Tomocube HT-2) microscopy. This advanced 3D imaging technique has been used to explore and understand the biology of many living cells and also microorganisms because of its advantage in that cells do not have to be stained, thus avoiding the interference of natural cell processes (Lee, Lee, Song, & Park, 2020; Oh, Ryu, Lee, & Park, 2020). As well, this microscopy can create 3D images of the studied cells. These advantages of using 3-dimensional holotomography enabled us to illustrate and compare the differences between the mature and immature DCs.

Materials and methods

Ethics approval and consent to participate

The cells used in this study were isolated from leukocyte concentrates (buffy coats) collected from healthy donors (n = 20) at the Blood Bank Center of Naresuan University Hospital. The study was approved by Naresuan University Institutional Review Board (IRB No.0045/62)

Isolation of human peripheral blood mononuclear cells and derivation of monocyte-derived dendritic cells

The peripheral blood mononuclear cells (PBMCs) were isolated from buffy coats by density gradient centrifugation on a Ficoll-Hypaque gradient (density 1.077 g/ml). The isolated PBMCs were cultured in complete RPMI-1640 medium (RPMI 1640 containing 10% heat-inactivated fetal calf serum (FCS), 100 U/ml penicillin, 100 µg/ml streptomycin, 10 mM HEPES and 2 mM L-glutamine, all from Gibco BRL, GB within a 37°C, 5 % CO_2 humidified incubator for 90 min in a tissue culture flask to isolate and collect adherent monocytes. The non-adherent cells were gently removed by pipetting out. Then, the obtained monocytes were cultured in a complete RPMI-1640 medium supplemented with 800 U/ml granulocyte-macrophage colony-stimulating factor (GM-CSF) (PeproTech, USA) and 500 U/ml interleukin-4 (IL-4) (PeproTech) for 6 days, with half of the culture medium refreshed every 2 days. Immature monocyte-derived dendritic cells (mDCs) were then able to be identified by the expression of cell surface molecules using flow cytometry. To produce mature mDCs, 5×10^6 immature mDCs were stimulated with lipopolysaccharide (LPS) 5 µg/ml (Sigma-Aldrich) and incubated for 48 hours (López-Relaño, Martín-Adrados, Real-Arévalo, & Martínez-Naves, 2018).

Antibodies

Antibodies used in this present study were as follows: CD14-PerCP (BioLegend, USA), CD80-APC (BioLegend), CD11c-PE, CD83-PerCP, CD86-APC, and HLA-DR-FITC (all from eBioscience, USA).

Flow cytometric analysis

The purity of the initially isolated monocytes was determined by CD14 expression. Both immature and mature mDCs were evaluated by their expression of CD80, CD11c, CD83, CD86, and HLA-DR. Cell surface molecules were analyzed using FACS Calibur (BD Biosciences, USA) with FlowJo software (Becton Dickinson, USA).

Three-dimensional images of living cells using a Tomocube Holotomography microscope

The morphology of immature and mature mDCs was analyzed using a holotomography (Tomocube HT-2) microscope. Upon analysis, mDCs ($5x10^4$ cells) were transferred to the glass-bottom Tomodish (Tomocube), and the 3D images created.

Intracellular lipid detection and analysis by Oil Red O staining method

Immature and mature mDCs ($1x10^5$ cells) were separately placed on slides, fixed by 10% formalin for 45 minutes, and then washed with running tap water. The slide was rinsed with 60% isopropanol for 5 min, stained with Oil Red O for 20 min, and then washed with deionized distilled H_2O (ddH_2O). The fixed cells were stained with hematoxylin for 1 minute and washed with ddH2O. Finally, the cells were inspected with an inverted microscope (Nikon Eclipse Ti-U, Nikon, Japan) and 3 photos were taken. The average % area of the lipid droplets was calculated using a digital image analysis program named Image J. This method was repeated 4 times for both immature and mature mDCs.

Statistical analysis

Data of the immature and mature mDCs were presented as mean ± SE. Statistics were performed using paired T-test and the Mann-Whitney U test. The p-values of less than 0.05 were considered statistically significant. All data were analyzed by using STATA (12.0) software.

Results

Isolation and culture of immature and mature dendritic cells

Monocytes isolated from PBMC were cultured with GM-CSF and IL-4 for 6 days to induce their differentiation into immature mDCs. Half of the immature mDCs were induced to maturity by stimulating with LPS for another 48 hr. Both immature and mature mDCs were identified by examining their expression of cell surface molecules. The immature mDCs expressed CD11c, CD80, and CD86, and were negative for CD14 (Figure 1A). The mature mDCs expressed a higher statistical intensity of CD80, and CD86 than the immature mDCs (Figure 1B). The results showed that the mature DCs expressed a significantly higher percentage of CD80 and CD86 (61% and 90%) than immature DCs (5% and 9%) (Figure 1C). The percentage of each surface molecule of both immature and mature DCs, assessed by flow cytometry is shown in Table 1.

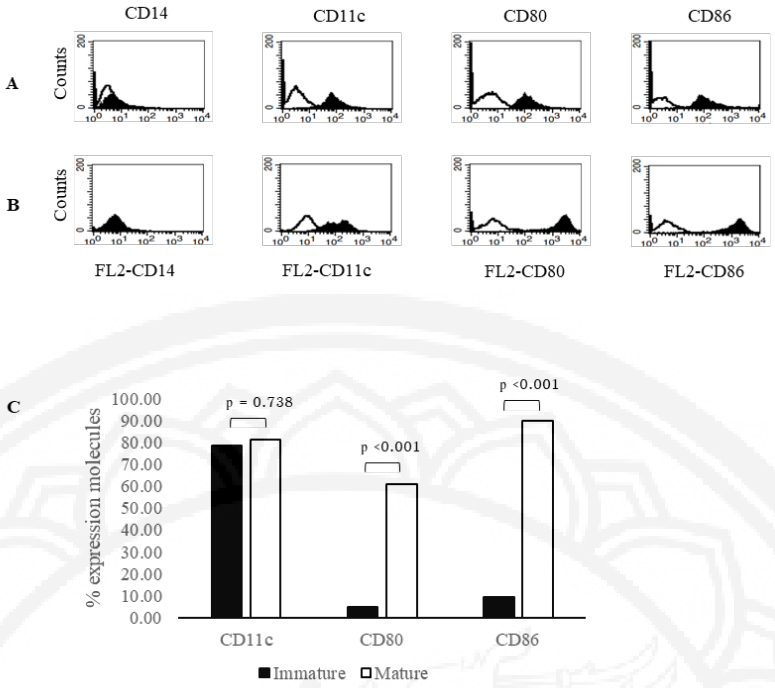

Figure 1 Phenotypes of immature and mature mDCs were demonstrated and identified by the expression of cell surface molecules. (A) Immature mDCs expressed CD11c, CD80, and CD86. (B) Mature mDCs were identified by higher expression of CD80 and CD86 compared to immature mDCs. (C) Mature mDCs expressed higher CD80 and CD86 than immature mDCs with a statistical significance ($p<0.001$)

Table 1 The percentage of surface molecules of both the immature and mature DCs

	Immature DCs			Mature DCs		
Buffy coat No.	%CD11c	%CD80	%CD86	%CD11c	%CD80	%CD86
B1	88.82	5.00	5.77	88.92	58.00	91.00
B2	73.14	6.88	8.21	74.27	53.47	89.86
B3	61.77	4.93	13.15	72.34	59.00	85.37
B4	90.00	2.34	10.70	89.67	74.03	92.82
average	78.43	4.79	9.46	81.30	61.13	89.76
STD	13.51	1.86	3.18	9.27	8.93	3.17

The illustrated results were from 4 buffy coats. All surface markers were shown as the percentage of expression using flow cytometry and also were calculated to show the average and standard deviation (STD).

Holotomography of immature and mature mDCs

We randomly took 3 immature and 3 mature mDCs, which were differentiated from one buffy coat sample, to inspect using a 3-dimensional Tomocube HT-2 microscope and compared the morphology and some indicative parameters: the refractive index and lipid concentration. The immature mDCs were flat with long pseudopods compared to mature mDCs (Figure 2 and 3, left column).

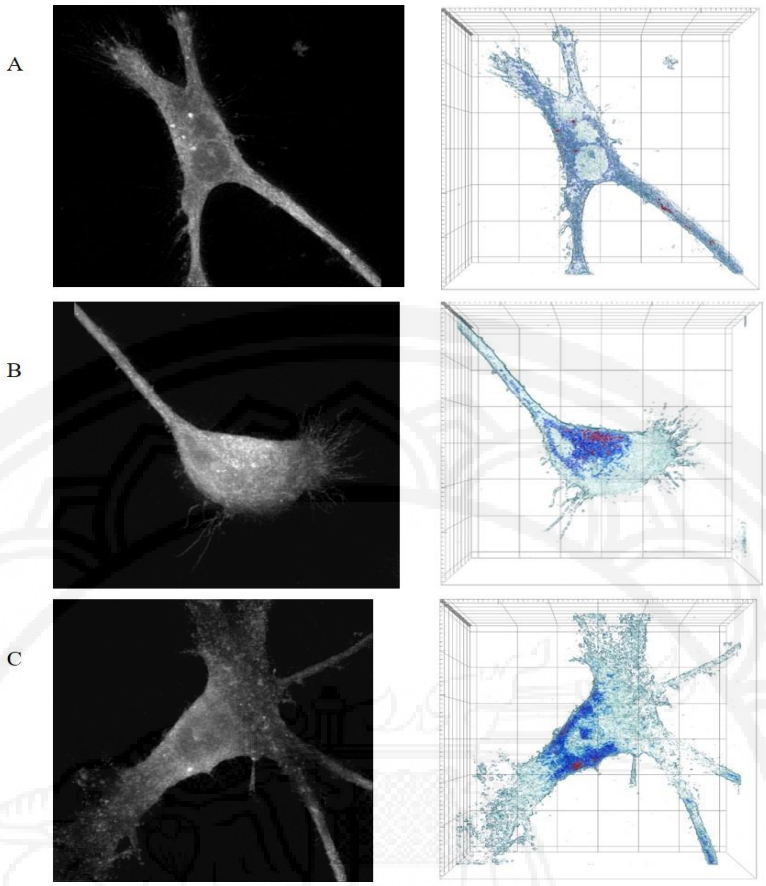

Figure 2 Label-free 2D and 3D images of three immature mDCs. Single frames from videos showed the whole image of immature mDCs acquired without any labeling (left column). The 3D image showed intracellular components in different colors (right column)

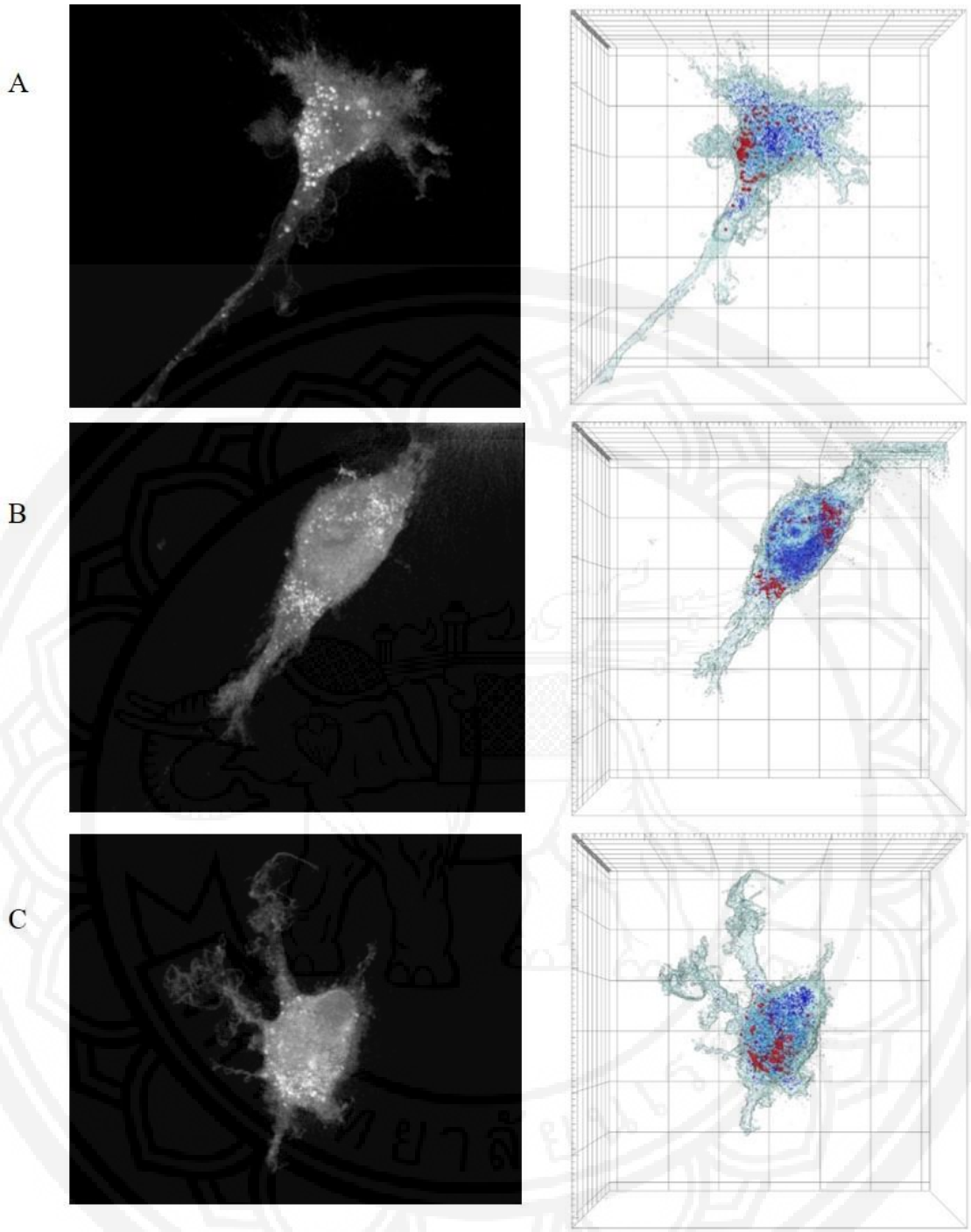

Figure 3 Label-free 2D and 3D image of three mature mDCs: The single video frame showed the image of mature mDCs acquired without any labeling (left column). The 3D image showed intracellular components in different colors (right column)

The results showed that the immature mDCs had a higher average cell volume (5657.93 μl) than the mature MDCs (4840.16 μl) (Figure 4A). However, this was not statistically significant (Table 2). The average cell mass of the mature mDCs (651.52 pg) was higher than the average cell mass of the immature mDCs (465.51 pg) (Figure 4B and Table 2). In addition, the cell mass per equal amount of volume was calculated to compare both stages of each mDC and found that the mature mDCs had a significant increase in cell mass (135.32 pg/μl) compared to the increase in cell mass in the immature mDCs (85.65 pg/μl) (Figure 4C).

Table 2 Cell volume and cell mass of immature and mature mDCs

	Cell volume (μl, n=3)	Cell mass (pg, n=3)
Immature mDCs	5657.93 ± 1618.89	465.51 ± 97.87
Mature mDCs	4840.16 ± 371.48	651.5 2 ± 43.34
p-value	0.513	0.158

Both cell volume and mass were represented as mean ± SD, calculated from 3 immature and 3 mature mDCs. The Mann-Whitney U test analyzed cell volume due to abnormal distribution of the dependent variable whereas cell mass was analyzed by the T-test. A p-value of <0.05 was considered significant.

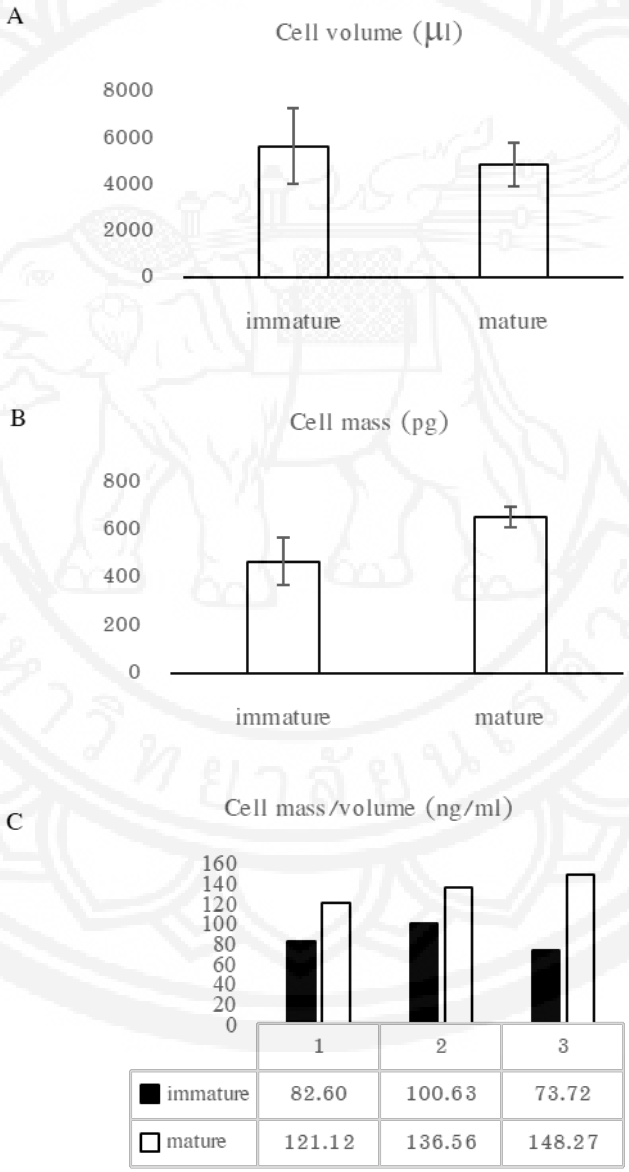

Figure 4 Cell volume and cell mass of immature and mature mDCs. 3 immature and 3 mature mDCs were analyzed for the average cell volume (A) and cell mass (B) and then presented as bar graphs. (C) The graph showed the cell mass per volume of each cell to confirm that the mature mDCs had increased cell mass compared to immature mDCs

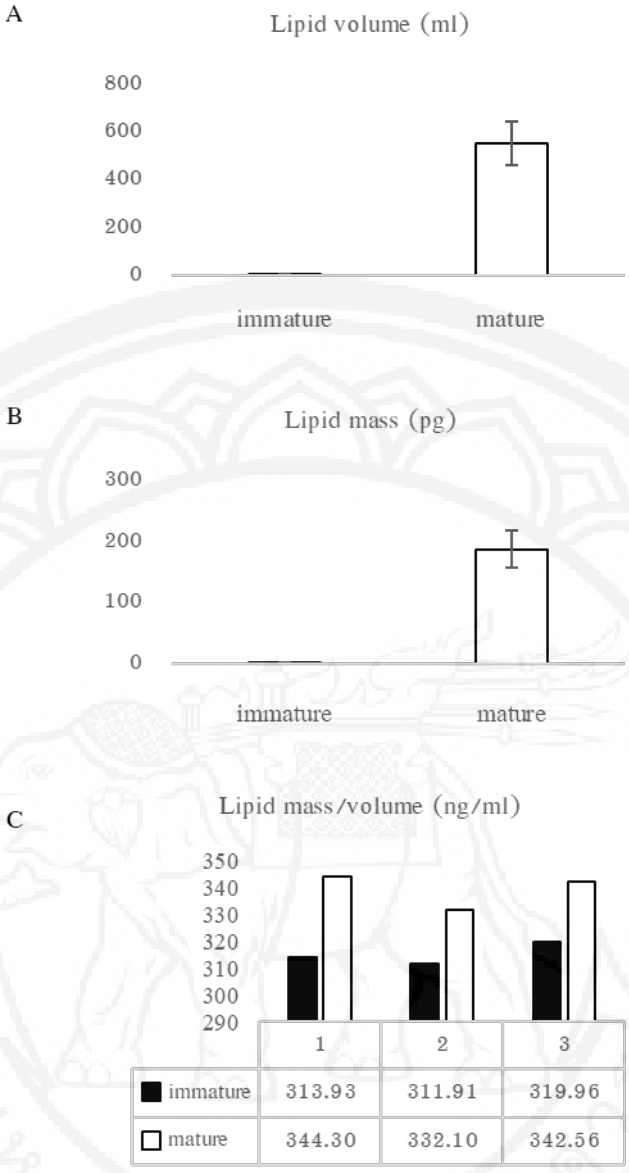

Figure 5 Lipid volume and lipid mass of immature and mature mDCs. 3 immature and 3 mature mDCs were analyzed for the average lipid volume (A) and lipid mass (B) and then presented as bar graphs. (C) the graph showed the lipid mass per volume of each cell to confirm that the mature mDCs had increased lipid mass compared to immature mDCs

In terms of indicative parameters, fewer bright white spots were identified as high refractive index droplets in immature mDCs (Figure 2 and 3, left column). These high refractive index droplets are shown in Figures 2 and 3, by red dots in the right column. This high refractive index was calculated and compatible with the lipid threshold refractive index, being equal to 1.3730 as previously reported by Park et al. (2020). Therefore, the mature mDCs had significantly more lipid mass and volume than the immature mDCs (Figure 5A, 5B, and Table 3). The intracellular lipid concentrations were calculated and each mature mDC was found to have a significantly higher amount of lipids than each immature mDC (Figure 5C). There was a much higher amount of intracellular lipids in the mature mDCs than in the immature mDCs detected by Oil Red O staining. The images of both cell types were taken and the area of each lipid droplet was calculated using the open-source ImageJ digital image analysis program (Figure 6). The results also showed that the mature mDCs had more

intense staining than the immature mDCs (Fig 6A and 6B). In addition, the analysis using the Image J software showed that the average % area of intracellular lipid in mature mDCs was higher than that in immature mDCs but had no statistical significance (Figure 6C).

Table 3 Lipid volume and lipid mass of immature and mature mDCs

	Lipid volume (μl, n=3)	Lipid mass (pg, n=3)
Immature mDCs	6.55±0.96	2.07±0.32
Mature mDCs	550.58±90.14	186.57±29.53
p-value	0.004	0.003

Both Lipid volume and mass were represented as mean ± SD, calculated from 3 immature and 3 mature mDCs. Lipid volume and lipid mass were analyzed by T-test. A p-value of <0.05 was considered significant.

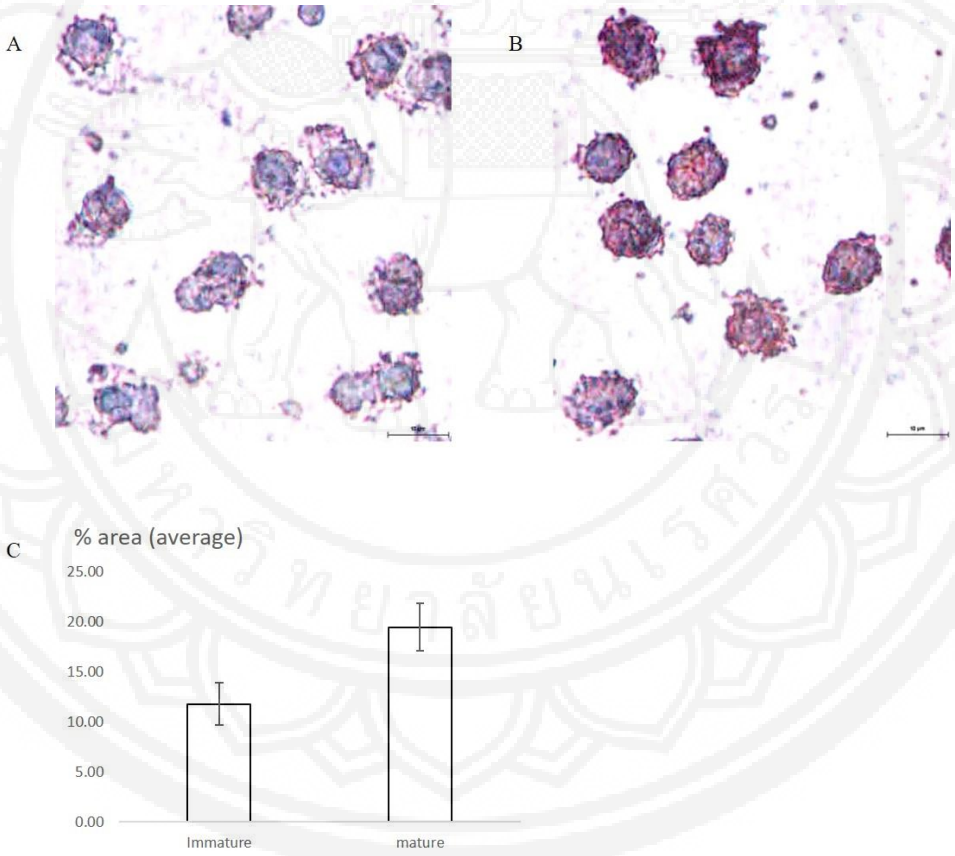

Figure 6 Immature (A) and mature mDCs (B) were stained with Oil Red O to determine the amount of intracellular lipid. They were visualized by inverted microscopy and the photos were taken. Photo (A) shows that the immature mDCs had less intense staining than the mature mDCs (B) which meant that the immature mDCs had a lower amount of intracellular lipid compared to the mature mDCs. (C) The bar graph showed the average of % area of intracellular lipid staining from images taken from both types of mDCs and analyzed by ImageJ software

Discussion

Dendritic cells are a very important component of the immune system. They function as antigen-presenting cells and are essentially involved in the mechanism of immunity to infection and cancer. The phenotype of mature and immature DCs has been demonstrated by many researchers in the past by using microscopy and the expression of cell surface molecules. With the detection of cell surface molecules using flow cytometry, we confirmed the higher intensity of CD80 and CD86 in mature mDCs than was found in previous studies (Lühr, Alex, Amon, & Dudziak, 2020; Poole et al., 2009; Morva et al., 2012). We demonstrated the morphology and some indicative parameters of both immature and mature mDCs by the recent technology, the Tomocube HT-2 microscope. This method helps to inspect the appearance of the single cells in three dimensions and also shows some intracellular components without damaging cells or disturbing normal molecular activities (Lambert, 2020). The mature mDCs had increased cell mass and lipid mass compared to immature mDCs. The increased lipid mass was confirmed by Oil Red O staining. The mature mDCs had more lipid mass than the immature mDCs which was also reported by Arai et al. (2018). This is opposed to the finding from Lühr et al. (2020), who reported no difference in lipid quantity but mature mDCs had increased phosphatidylcholine and decreased sphingomyelin compared to immature cells. However, limited data are available on the intracellular lipid change accompanied by the expression of costimulatory molecules (CD80 and CD86) and thus more studies are needed.

That the mature mDCs have an increased cell mass may be associated with the increased lipid mass in the cells as the lipids are important energy storage for the cells (van Meer, Voelker, & Feigenson, 2008). In addition, changing the lipid components of mammalian cell membranes may facilitate signaling into the cell and may involve the immune function of mDCs. The increased accumulation of lipids in mature mDCs may influence the function of dendritic cells in activating T cell response. One previous animal study reported that mice with cancer had higher lipid accumulation in the DCs than normal mice. This lipid accumulation in cancer host DCs is related to increased expression of macrophage scavenger receptor1 (Msr1) and a defect in an antigen-presenting process to T cells (Herber, Cao, Nefedova, & Gabrilovich, 2010). Therefore, the effects of lipid accumulation and metabolism in DCs need to be further investigated.

Conclusion

In conclusion, our study demonstrated the morphological features and intracellular lipid changes of the immature and mature mDCs using 3D tomographic microscopy. This type of imaging could help us to gain more information on intracellular components, such as lipids and proteins using calculated the reflective index. This would open a new avenue for further research into the function of immune cells and the relationship of the metabolism at the various stages of these cells.

Acknowledgements

We would like to thank Mr. Supakorn Sirinutsomboon and Ms. Sudarat Iemtod (Hollywood International Group, Bangkok, Thailand) for operating the Tomocube microscopy, and also Ms. Pattamaphorn Phunsomboon, Ms. Jeeranan Jantra, and Ms. Kwansuda Supalap for technical assistance. Also, we thank Mr. Roy I. Morien of

the Naresuan University Graduate School for his editing of the grammar, syntax and general English expression in this manuscript.

Funding statement

This project is funded by the National Science Research and Innovation Fund (NSRF) (grant no. R2564B033 to AW and R25265B001 to SP). Sutatip Pongcharoen's project is also funded by the National Research Council of Thailand (NRCT) and Naresuan University: N42A650331.

References

Andreae, S., Piras, F., Burdin, N., & Triebel, F. (2002). Maturation and activation of dendritic cells induced by lymphocyte activation gene-3 (CD223). *Journal of immunology*, *168*(8), 3874-3880.

Arai, R., Soda, S., Okutomi, T., & Ishii, Y. (2018). Lipid Accumulation in Peripheral Blood Dendritic Cells and Anticancer Immunity in Patients with Lung Cancer. *Journal of immunology research*, *2018*, 5708239.

Banchereau, J., & Palucka, A. K. (2005). Dendritic cells as therapeutic vaccines against cancer. *Nature reviews. Immunology*, *5*(4), 296-306.

Constantino, J., Gomes, C., Falcão, A., Cruz, M. T., & Neves, B. M. (2016). Antitumor dendritic cell-based vaccines: lessons from 20 years of clinical trials and future perspectives. *Translational research: the journal of laboratory and clinical medicine*, *168*, 74-95.

Herber, D. L., Cao, W., Nefedova, Y., & Gabrilovich, D. I. (2010). Lipid accumulation and dendritic cell dysfunction in cancer. *Nature medicine*, *16*(8), 880-886.

Kim, M. K., & Kim, J. (2019). Properties of immature and mature dendritic cells: phenotype, morphology, phagocytosis, and migration. *RSC Advances*, *9*, 11230-11238.

Lambert, A. (2020). Live Cell Imaging with Holotomography and Fluorescence. *Microscopy Today*, *28*(1), 18-23.

Lee, M., Lee, Y. H., Song, J., & Park, Y. (2020). Deep-learning-based three-dimensional label-free tracking and analysis of immunological synapses of CAR-T cells. *eLife*, *9*, e49023.

López-Relaño, J., Martín-Adrados, B., Real-Arévalo, I., & Martínez-Naves, E. (2018). Monocyte-Derived Dendritic Cells Differentiated in the Presence of Lenalidomide Display a Semi-Mature Phenotype, Enhanced Phagocytic Capacity, and Th1 Polarization Capability. *Frontiers in immunology*, *9*, 1328.

Lühr, J. J., Alex, N., Amon, L., & Dudziak, D. (2020). Maturation of Monocyte-Derived DCs Leads to Increased Cellular Stiffness, Higher Membrane Fluidity, and Changed Lipid Composition. *Frontiers in immunology*, *11*, 590121.

Morva, A., Lemoine, S., Achour, A., Pers, J. O., Youinou, P., & Jamin, C. (2012). Maturation and function of human dendritic cells are regulated by B lymphocytes. *Blood*, *119*(1), 106-114.

Oh, J., Ryu, J. S., Lee, M., & Park, Y. (2020). Three-dimensional label-free observation of individual bacteria upon antibiotic treatment using optical diffraction tomography. *Biomedical optics express*, *11*(3), 1257-1267.

Park, S., Ahn, J. W., Jo, Y., Kang, H. Y., Kim, H. J., Cheon, Y., ... Park, K. (2020). Label-Free Tomographic Imaging of Lipid Droplets in Foam Cells for Machine-Learning-Assisted Therapeutic Evaluation of Targeted Nanodrugs. *ACS nano*, *14*(2), 1856-1865.

Poole, J. A., Thiele, G. M., Alexis, N. E., Burrell, A. M., Parks, C., & Romberger, D. J. (2009). Organic dust exposure alters monocyte-derived dendritic cell differentiation and maturation. *American journal of physiology. Lung cellular and molecular physiology*, *297*(4), L767-L776.

Randolph, G. J., Jakubzick, C., & Qu, C. (2008). Antigen presentation by monocytes and monocyte-derived cells. *Current opinion in immunology*, *20*(1), 52-60.

Steinman, R. M. (2007). Lasker Basic Medical Research Award. Dendritic cells: versatile controllers of the immune system. *Nature medicine*, *13*(10), 1155-1159.

Thurnher, M. (2007). Lipids in dendritic cell biology: messengers, effectors, and antigens. *Journal of leukocyte biology*, *81*(1), 154-160.

van Meer, G., Voelker, D. R., & Feigenson, G. W. (2008). Membrane lipids: where they are and how they behave. *Nature reviews. Molecular cell biology*, *9*(2), 112-124.

Verdijk, P., van Veelen, P. A., de Ru, A. H., Hensbergen, P. J., Mizuno, K., Koerten, H. K., ... Mommaas, A. M. (2004). Morphological changes during dendritic cell maturation correlate with cofilin activation and translocation to the cell membrane. *European journal of immunology*, *34*(1), 156-164.

Xing, F., Wang, J., Hu, M., & Liu, J. (2011). Comparison of immature and mature bone marrow-derived dendritic cells by atomic force microscopy. *Nanoscale research letters*, *6*(1), 455.